

FLUID FLOW IN THE MELT OF SOLIDIFYING MONOTECTIC ALLOYS

DEC 10 1989

A. Ecker *, J. I. D. Alexander **, D. O. Frazier

(NASA-TM-101786) FLUID FLOW IN THE MELT OF
SOLIDIFYING MONOTECTIC ALLOYS (NASA.
Marshall Space Flight Center) 25 p

N89-71080

Unclas

00/26 0213160

Space Science Laboratory, NASA/Marshall Space Flight Center
Huntsville, Alabama 35812

* ESA Visiting Scientist, ** USRA Visiting Scientist

INTRODUCTION

The microstructure of cast metallic materials is largely determined by the primary solidification phenomena which are influenced by fluid flow conditions in the melt. In order to optimize the properties of the castings, comprehensive knowledge is required of the interaction between temperature and concentration dependent layers close to the solidification front and fluid flow in the melt. Transparent model systems which solidify in the same manner as metals can be effectively utilized for fundamental investigations because they allow in-situ observation of the environment close to the solid-liquid interface.

The objective of this work is to investigate the interactions between temperature, concentration and fluid flow at 1g and 10^{-4} g conditions in the melt adjacent to the solid-liquid interface in metallic alloys using transparent solidifying monotectic model systems. One major point of interest is the simultaneous measurement of the temperature, concentration and fluid flow induced by the interaction of the different phenomena in a solidifying monotectic melt. The "Two Wavelength Holography" method provides the opportunity to measure temperature and concentration directly simultaneously.

TRANSPARENT MONOTECTIC MODEL SYSTEMS

Two succinonitrile based alloy systems which solidify in the same manner as metals were studied. Figure 1 shows the phase diagram of succinonitrile-ethanol (SCN-E) and succinonitrile-water (SCN-W). Both are miscibility gap systems. One important difference between the solidification front dynamics of these systems is the difference in wetting characteristics between liquid (2) and the solid. If liquid (2) wets the solid matrix the system solidifies with a stable growing interface (system SCN-W). If the solid matrix will not be wet by the liquid (2) the system solidifies with an unstable interface (system SCN-E). Through experiments, an empirical separation parameter $T_M/T_C > \text{or} < 0.9$ was developed by Grugel et al. [4] where T_M = monotectic temperature and T_C = critical temperature. Based on these experimental results, systems with

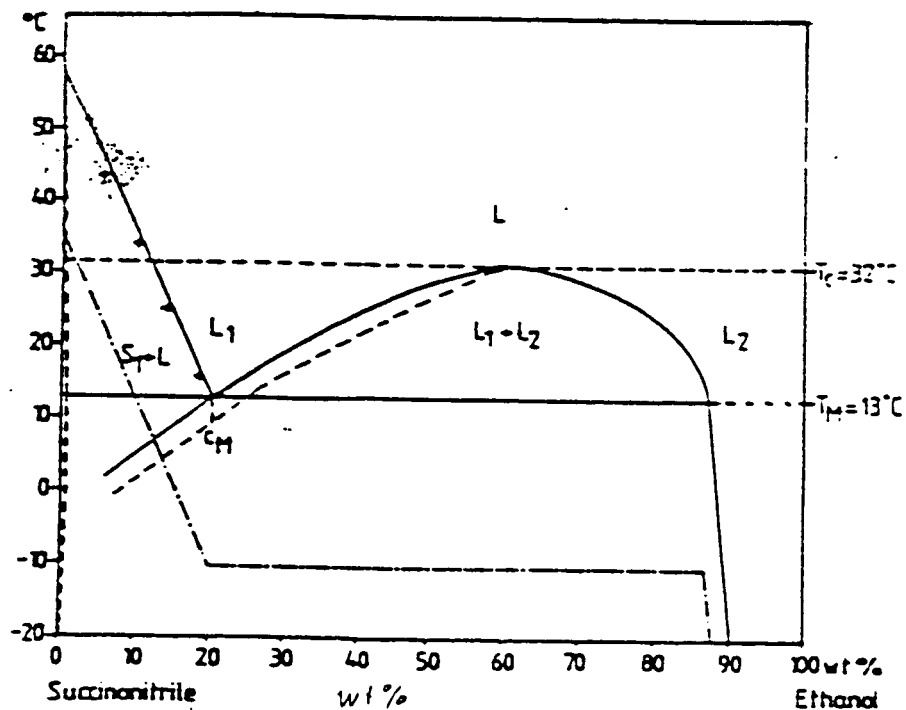
$$T_M/T_C < 0.9$$

grow stable. Systems with

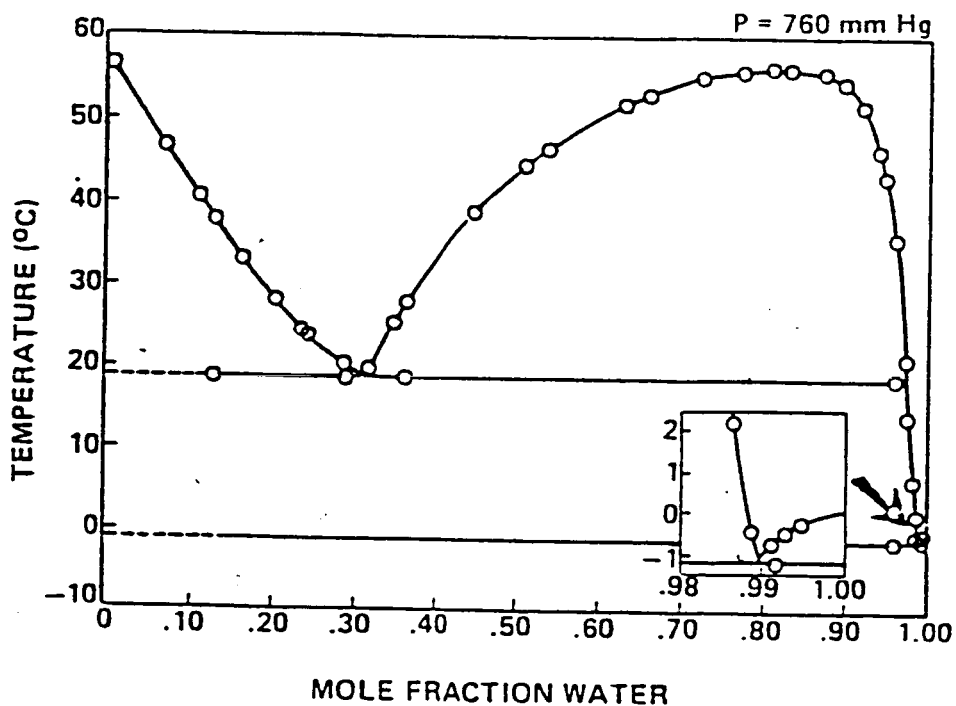
$$T_M/T_C > 0.9$$

grow unstable, fig. 2.

Different wetting properties at the monotectic trijunction will cause different phase separation during monotectic solidification. The thermodynamics of phase decomposition will not be



(a)



(b)

Figure 1: Phase diagram of monotectic model alloys; Succinonitrile-Ethanol (SCN-E) based on measurements by Schreinemakers [1] and Ecker [2] (a); Succinonitrile-Water (SCN-W) based on measurements by Schreinemakers [1] and Smith et al. [3] (b).

influenced.

THERMODYNAMICAL AND FLUID MECHANICAL PROCESSES IN THE MELT

The fluid flow in the melt in front of a solidifying monotectic alloy will be driven by either thermocapillary or buoyancy forces.

Thermocapillary driven convection occurs when the "surface tension" of a deformable interface is a function of the local temperature of that interface. For droplets with a surface tension that is a decreasing function of temperature, the presence of a temperature gradient will result in the motion of the droplet toward the higher temperature [5].

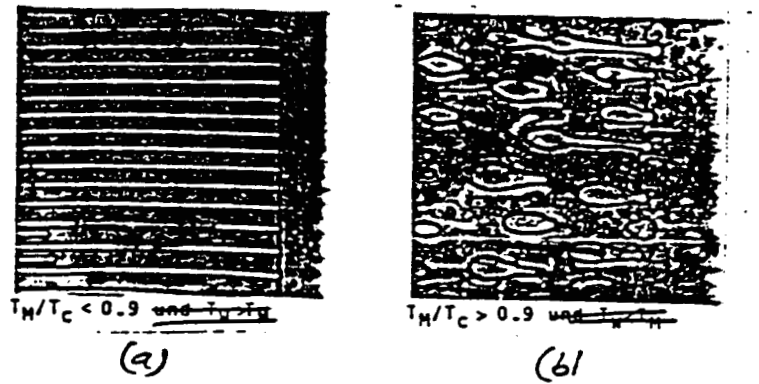
Whenever such motions occur in the systems under investigation here, they will be either ~~be~~ augmented or diminished by buoyancy forces caused by density difference between the droplet phase (L_1, L_2) and the enveloping liquid phase. In particular, for SCN-rich droplets in a W-rich liquid, buoyancy effects will retard the thermocapillary driven motion whereas for W-rich droplets in a SCN-rich liquid buoyancy will enhance the thermocapillary driven motion.

In the neighborhood of the solid-liquid interface, volumes of liquid can be created that ~~are~~^{are} less dense than the surrounding melt. This will result in the vertical buoyant motion of the volume provided that the gravity body force vector points into the solid phase. In addition to the above, the systems examined here also admit the possibility of thermosolutal convection since the mass density of the melt is a function of both temperature and concentration [6].

PHASE SEPARATION IN THE MELT

A known mechanism inducing phase separation in miscibility gap type systems is droplet migration in a thermal gradient resulting from the fact that surface tension varies with the temperature. A first-order theory was developed by Young, Goldstein and Block (YGB) [5]. The theory predicts that gas bubbles or other fluid second-phase droplets will migrate with a rate that is proportional to the product of the radius, the derivative of the interfacial tension with respect to temperature, and the thermal gradient. If the interfacial tension decreases with increasing temperature, which is the case for most materials, the droplets of the minority phase will migrate in the direction of the thermal gradient. This droplet motion creates a high amount of heat and mass transport between the area in front of the solid-liquid interface and the melt.

The experimental test of the theory performed by YGB consisted of balancing the Stokes' motion of the particles in silicone oil



(a) stable monotectic
solidification of SCN-2.5 wt%
Glycerol

(b) unstable monotectic
solidification of SCN-
20 wt% Ethanol

Figure 2: The experimentally determined relationship [4] between the monotectic (T_M) and critical (T_C) temperatures; stable growing monotectic structure (a) and unstable growing monotectic structure.

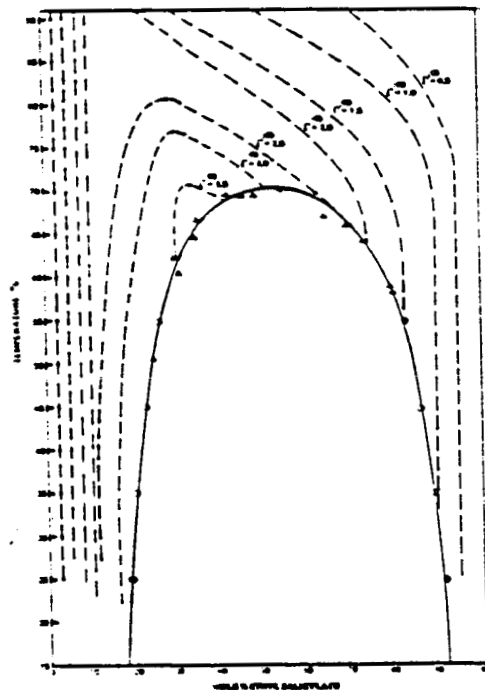


Figure 3: Phase diagram of the monotectic model alloy Diethylene Glycol - Ethyl Silicate, Smith et al. [7].

against the thermocapillary forces that result from a vertical thermal gradient. The situation is somewhat different in a liquid-liquid system, however, especially when solubility varies appreciably with temperature. In order to test the applicability of the YGB theory to a monotectic system (two-phase region), Lacy et al. [7] performed an experiment using a diethylene glycol (DEG) and ethyl silicylate (ES) solution, fig. 3. The purpose of the measurement was to see how well the YGB theory applied to the two-phase region of a monotectic system. There was considerable scatter in the data due to the difficulty in measuring the particle diameter and velocity from the photographs, and to uncertainties in the temperature field in the vicinity of the droplet. The difference between measured and theoretical results was -31.9 to +13.8 percent.

More recently a considerable effort has gone toward observing directional solidification in another miscibility-gap type system, SCN-W [Frazier et al. [8]]. Below about 42°C, the SCN-rich phase is the denser phase. At 42°C the SCN-rich phase becomes the less dense phase up to the critical temperature at 56.1°C. W-rich solutions having consolute temperatures below 42°C were directionally solidified at approximately 2 cm/hr. With a thermal gradient of about 17 K/cm, droplets of radii $R = 0.5$ mm at velocities $v = 4$ mm/s originate near the solid-liquid interface and move upward to the hot zone and dissolve above the consolute isotherm. Very small droplets from near the consolute isotherm fall toward the solid-liquid interface in columns parallel to the path of the rising larger droplets. This gives the odd appearance of large droplets rising in a counter-current of falling smaller droplets. Both streams must differ considerably in concentration from the surrounding water-rich melt, since they are clearly separated by sharp interfaces and there have to be counter-flowing fluid streams which transport the droplets. Presumably, the rising droplets are succinonitrile-rich, hence heavier than the surrounding water-rich melt (below 42°C), and therefore rising due to thermal migration to minimize interfacial tensions. From these considerations, the origin of the smaller, falling droplets has to be determined.

PHASE SEPARATION THROUGH THE MONOTECTIC SOLIDIFICATION

The first experiment using an interferometric measurement technique to determine the concentration and temperature distribution in the monotectic system at 1g and micro-g involve the hypomonotectic system succinonitrile-ethanol [Sahm and Ecker [9]; Ecker [2]]. In contrast to results from the microgravity experiment, earth based experimental results showed disturbances in the heat flow as well as in the diffusion profiles, fig. 4. Using an interferometric technique and thermocouples in the melt revealed the development of a concentration maximum in the system. If the initial concentration of the solution was between 12-22 wt% E a

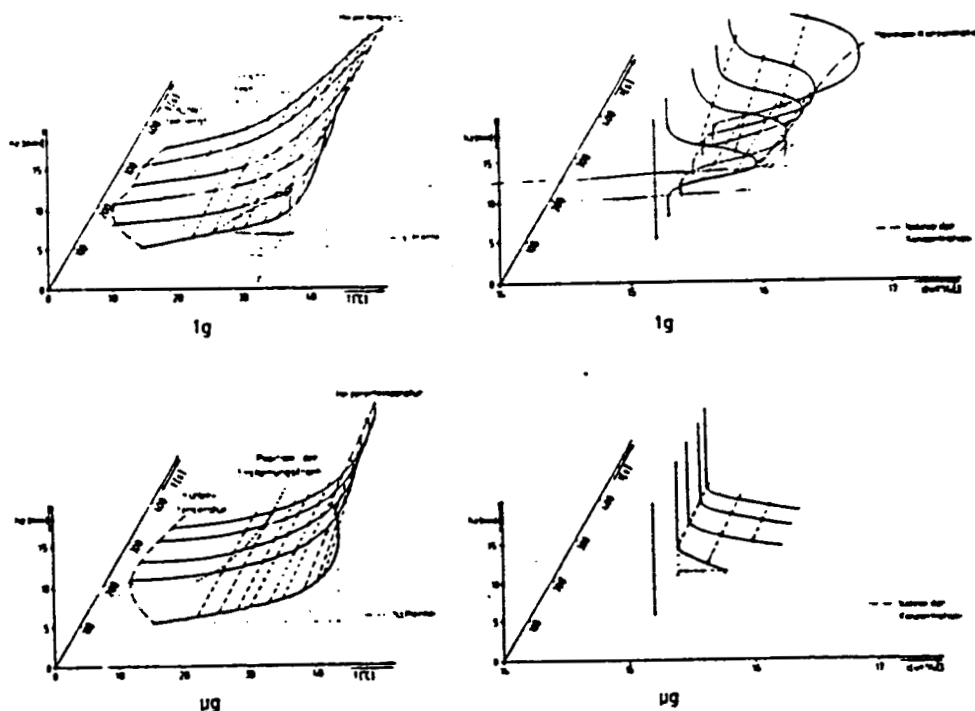


Figure 4: Concentration and temperature profile of the 1g and micro-g TEXUS-10 experiment GTS ("Boundary layers at transparent solidifying melts") with SCN-E. Under micro-g conditions the temperature profile will be dependent on diffusion alone. The concentration layer in front of the solid-liquid interface corresponds to the well known theory ($\delta_c \approx 2 \cdot D/v$). Under 1g the temperature profile differs from the pure thermodiffusion profile. Also small rising droplets, which will be resolved at the critical temperature ($T_c = 32^\circ\text{C}$) change the temperature and concentration profiles in the melt. A concentration maximum was found at the 32°C isotherm in the melt.

concentration maximum occurred at the critical temperature isotherm T_C . This concentration peak was notable after supercooling the melt under the extended consolute curve before the solidification started. This supercooling will be reduced rapidly by the growing solidification front. Without this undercooling this concentration peak still increased and did not disappear as assumed. This was the first indication of a phase separation in the hypomonotectic region induced by the monotectic solidification front. Owing to buoyancy differences and thermocapillary forces, it is possible for the L_2 phase to leave the solid-liquid interface, fig. 5. If there is additionally a non-wetting condition between S_1 and L_2 , the degree of phase separation seems to be only a function of the solidification velocity. At high velocities only small droplets can leave the interface. Larger droplets will be incorporated by the advancing solid. These can escape entrapment by the advancing interface only at very low growth rates, fig. 6.

With the interferometric technique only the disturbances caused by large droplets can be measured directly. These will only be visible toward the end of the experiment at lower solidification rates. In comparison, reduced gravity conditions, such as those which prevailed during the sounding rocket experiment TEXUS-10, lead to concentration boundary layers ahead of the solidification front, fig. 7. Both, the ground based and the sounding rocket experiment TEXUS-10 were started with a high solidification velocity ($v_s = 10^{-2}$ mm/s). At the end of the experiment the velocity was only $v_s = 5 \cdot 10^{-5}$ mm/s. At this velocity larger interferometric measurable droplets migrate under lg conditions.

The causes of fluid flow in monotectic systems in the vicinity of the solidification front during earth laboratory experiments are summarized below:

- a) Separation processes in the melt below the consolute temperature.
- b) Dynamic processes at the liquid (1) - liquid(2) - solid (1) trijunction (wetting conditions).
- c) Solidification velocity.
- d) Thermocapillary driven motion resulting from thermal and solutal differences in the interface.
- e) Density differences between the liquid (1) - liquid (2).

TWO WAVELENGTH HOLOGRAPHY

Droplets move owing to buoyancy and thermocapillary forces. Consequently, the temperature and concentration of the melt and of the droplets change continuously due to diffusion and the resulting fluid motion. A Mach-Zehnder interferometric technique used to measure the concentration and temperature changes in front of a solid-liquid interface could only provide limited information

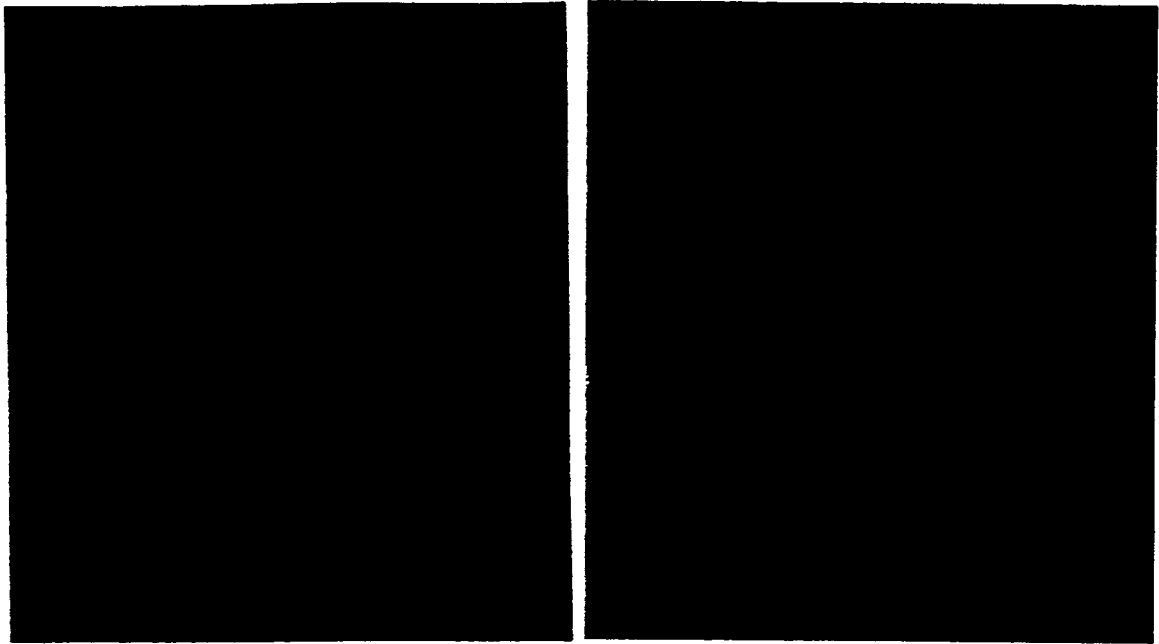


Figure 5: Phase separation driven by the interdendritic monotectic solidification. From the unstable growing monotectic phase (alloy: SCN-12wt%E) E-rich droplets with the radius $R=0.05$ mm and velocities of $v_D=0.5$ mm/s start rising into the melt until they will be resolved near the critical isotherm.

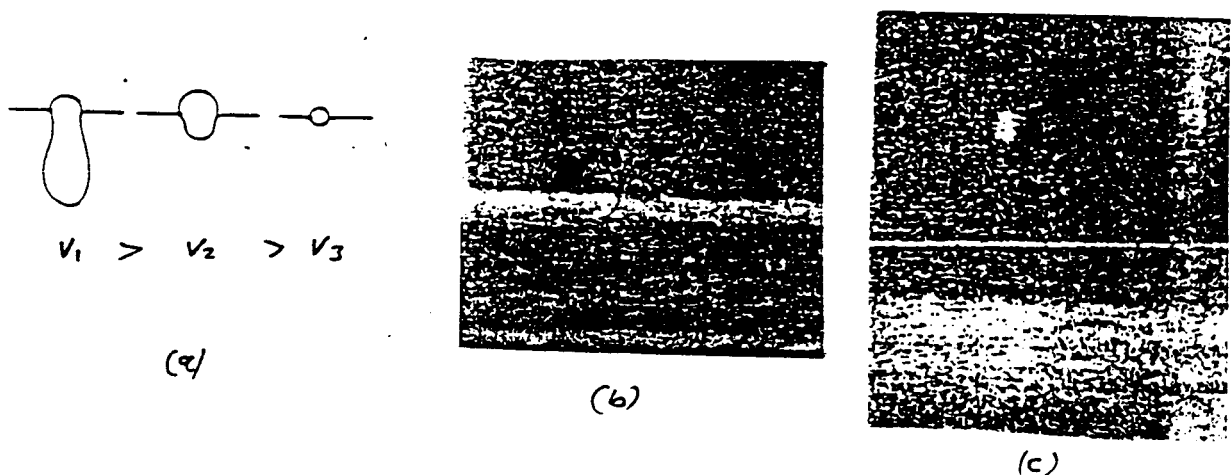


Figure 6: Whether a solidifying interface incorporates or pushes droplets depends on the wetting conditions between S_1 and L_2 and of the solidification velocity. If L_2 does not wet S_1 (SCN-E) then growth the monotectic phase with a similar structure as showed at (a); large solidification velocities lead to an incorporation of droplets (b), smaller velocities to rising droplets (c).

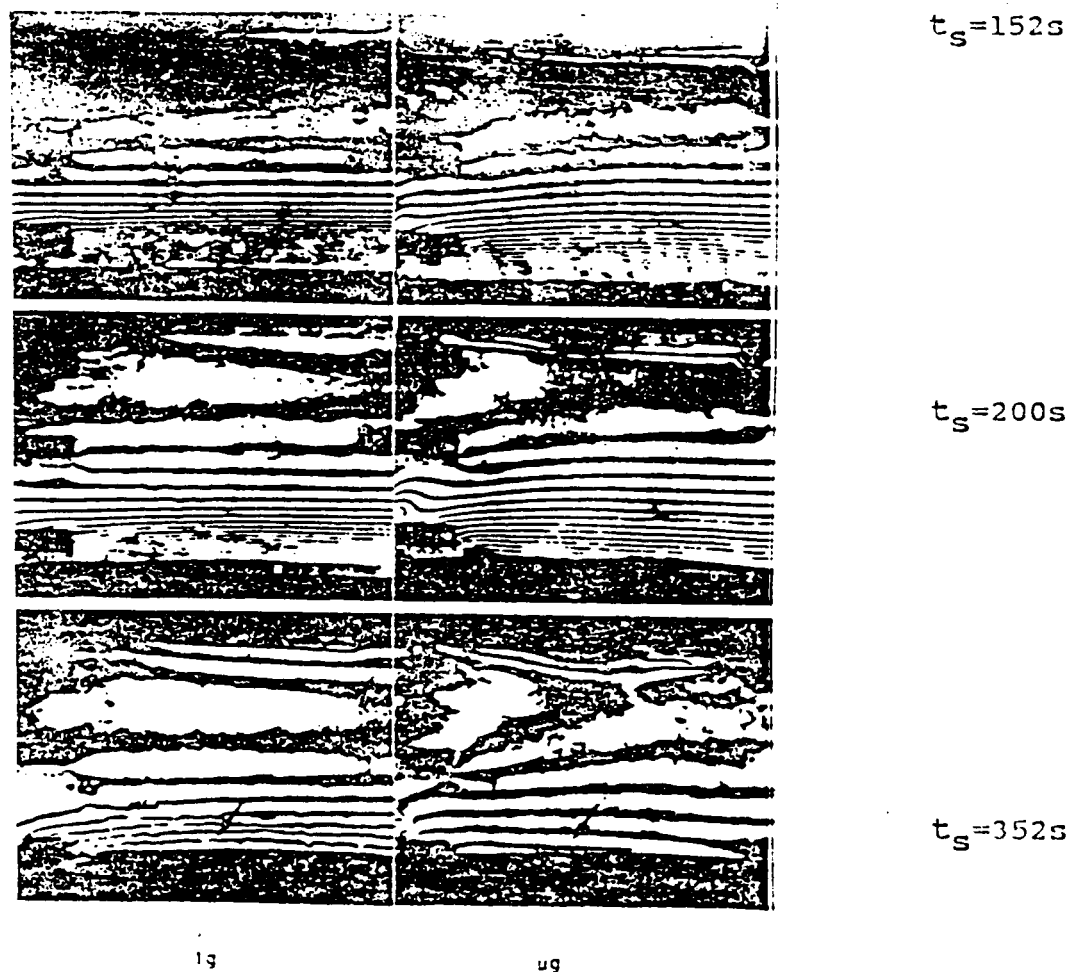


Figure 7: The comparison between the interferograms of the micro-g TEXUS-10 rocket experiment and the lg reference experiment at three times demonstrates the different fluid motion in the melt. The pure thermodiffusion profile at the lg experiment will be disturbed directly in front of the solid-liquid interface.

about the refractivity changes in the melt. Since the refractive index is a function of the temperature and concentration, there has to be additional information for the evaluation of the interferograms. In the field of solidification front dynamics, measurements of the temperature profile previously relied on the use of thermocouples. This only provides local information of the temperature profile. The influence of the fluid flow has to be neglected. In order to increase the accuracy of the result the density profiles have to be monitored by an interferometric method which will allow the separation of temperature and concentration profiles without measurement of the temperature by thermocouples in the melt. The "Two Wavelength Holographic Technique" provides such a possibility. The accuracy of the measurements is as high as that obtained using standard holographic technology. The two wavelength holographic method is transferable to any optical system, fig. 8.

The two wavelength technique was used years ago by Ross and El-Wakil [10] and by Mayinger and Panknin [11] to measure separately the temperature and concentration of a burning fuel drop. This technique offers a significant opportunity to determine the temperature and concentration profiles simultaneously in all processes where heat and mass transport in transparent systems occur. Each wavelength is reconstructed separately and each reconstruction contains the information on temperature and concentration changes. Since the refractivity is a function of the wavelength, it is possible to determine both profiles from the differences between the holograms, fig. 9.

Initial information from the holograms are changes in the optical path through the sample (table 1, equation 1). Here, s is the interference order in multiples of the different wavelength λ_j and λ_k . Equation 1 can be integrated, if the intensity of the total field is constant. For fluids, the Lorentz-Lorenz equation gives the relation between the refractivity n , the refractive index R , and the density of the melt (equation 2). The slope of the fringe shift depends on the change of the refractivity between both exposures. Since temperature and concentration profile information are in both reconstructions, it is possible to eliminate concentration in one of both equations and solve it (equation 3) for the temperature profile. Using this temperature profile, the concentration profile may be determined by equation 4. More about this technique will soon be published elsewhere.

EXPERIMENTAL RESULTS AND DISCUSSION

Using different optical measurement techniques such as shadow-graph, one- and two-wavelength holography, or microscopy it is possible to determine the nature of fluid flow in the melt, which are characteristic of various alloy concentrations. To separate the phenomena, there were careful investigations in seven regions

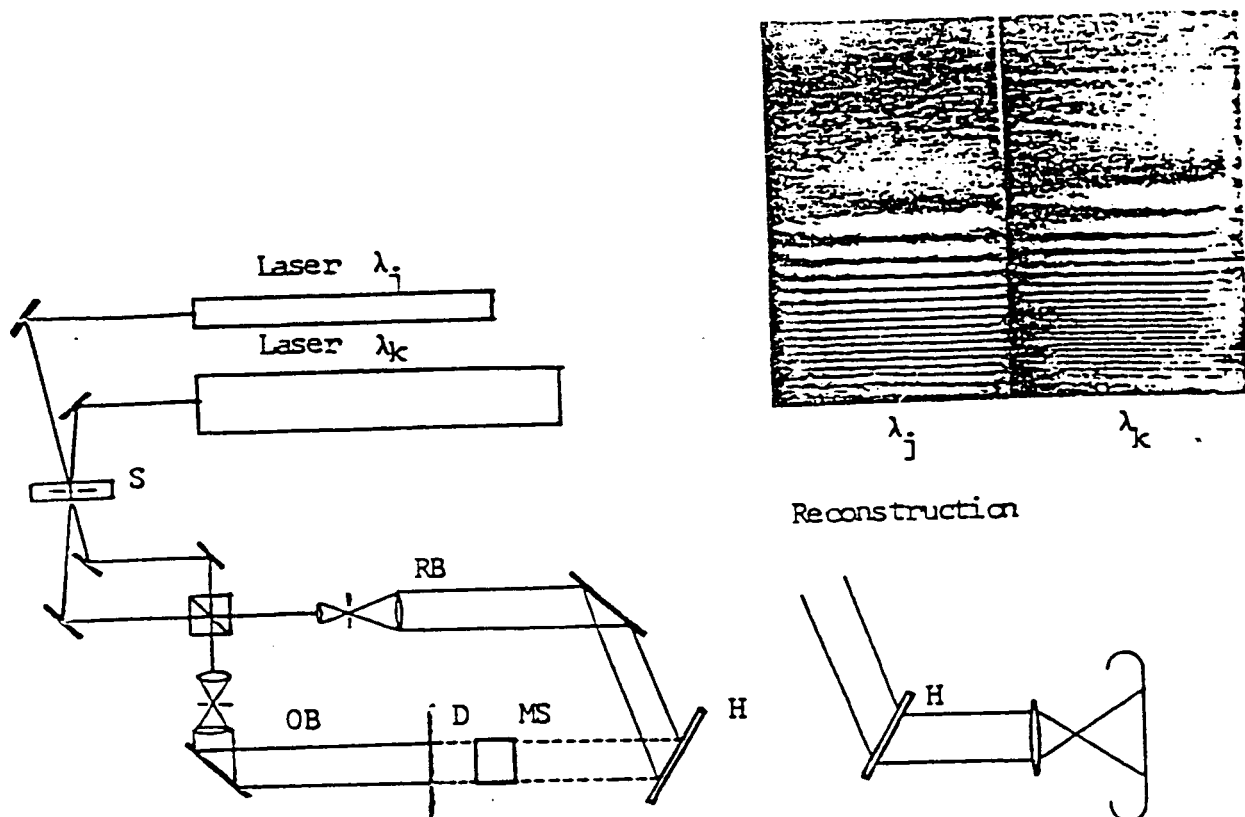
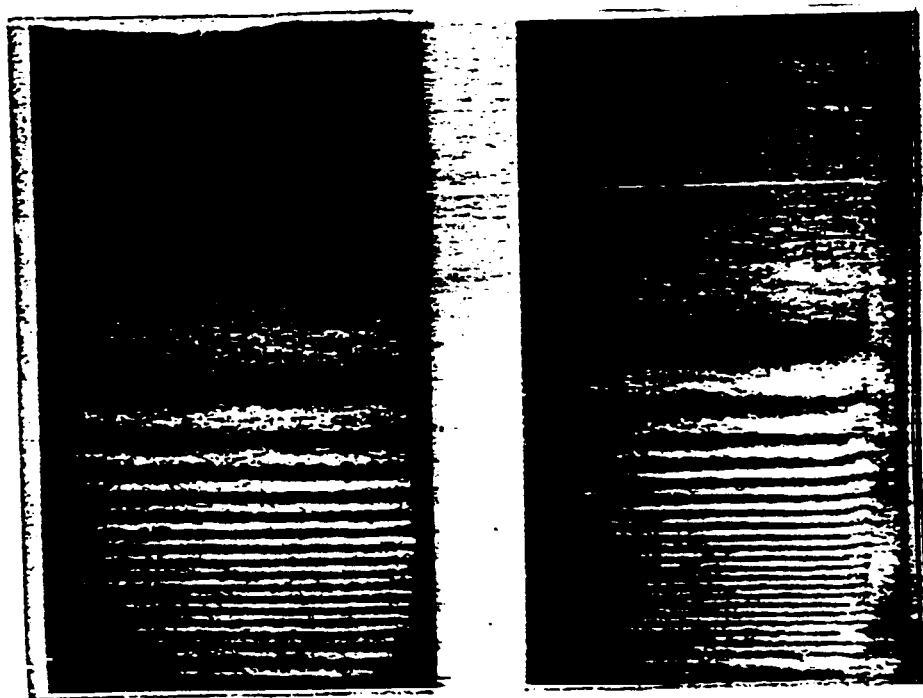


Figure 8: Principle set-up for the Two Wavelength Holographic device, first used by El-Wakil and Ross [10].



(a)

(b)

Figure 9: Reconstruction of a Two Wavelength Hologram of Laser and an Argon Laser. Both reconstructions show the same temperature changes (a), or the same concentration changes (b). The number of fringes observed differs about 30%.

Table 1: Basic Evaluations for Two Wavelength Holography

$$(1) \quad s \cdot \lambda = \int_s (n_1 - n_2) \cdot ds$$

$$(2) \quad \frac{n(T, c)^2 - 1}{n(T, c)^2 + 2} = R(\lambda) \cdot (T, c)$$

$$(3) \quad \frac{dT}{dy} = \frac{\partial n_k / \partial c \cdot ds_j / dy \cdot \lambda_j / l - \partial n_j / \partial c \cdot ds_k / dy \cdot \lambda_k / l}{\partial n_k / \partial c \cdot \partial n_j / \partial T - \partial n_k / \partial T \cdot \partial n_j / \partial c}$$

$$(4) \quad \frac{dc}{dy} = \frac{ds_k / dy \cdot \lambda_k / l - \partial n_k / \partial T \cdot dT / dy}{\partial n_k / \partial c}$$

with: l = sample depth, s = fringe number, λ = wavelength (λ_j = 488 nm, λ_k = 632.3nm), n = refractivity $f(\lambda, T, c)$, R = refractive index, c = concentration, T = temperature

of the monotectic phase diagrams, SCN-E and SCN-W, fig. 10.

For the following measurements the temperature gradient G_T was always chosen so that the solidification took place with constitutional supercooling.

In regions I and VII, the minority phase can be incorporated completely in the solidifying majority phase. Growing dendrites from this region are shown in fig. 11.

In regions VI, a eutectic interdendritic phase will grow. At the eutectic solidification both components between the primary dendrites are solid.

Fluid flow in the melt of solidifying alloy compositions at regions I, VI and VII with a stabilizing temperature gradient can only occur if there is high supersaturation of the less dense material in front of the advancing interface (thermosolutal convection).

This behavior changes completely at region II. High under-coolings under the extended consolute curve could lead to thermodynamic decomposition of the melt. Droplets of phase L_2 migrate, driven upward, by thermocapillary and buoyancy forces, toward the high temperature region.

A monotectic phase grows between the primary solidifying dendrites. The solidifying monotectic separates the melt L into L_2 and S_1 . For unstable growing monotectics L_2 does not wet the S_1 phase. Since this phase is readily detached from the interface it is able to move ahead of the growing solid as a result of thermocapillary and buoyancy effects, fig. 12. *incorp*

only It is important to note that at high solidification velocities ($6 \cdot 10^{-3}$ mms $^{-1}$) only small droplets (radius $2 \cdot 10^{-2}$ mm) are observed [2,12]. At lower solidification velocities larger droplets have sufficient time to move ahead of the solid. The reason that small droplets are favored at high solidification rates is that detachment of small droplets from the solid requires less force and less time than for larger droplets. *large droplets are favored at lower solidification rates*

Each tail behind rising droplets contains a higher concentration of the minority phase. The low number of migrating droplets may not stabilize a plume-like structure in the melt. The resulting fluid flow in the melt changes its thermal and solutal conditions significantly. *a higher solidification rate*

In comparison to the lg measurements, results from a TEXUS-10 sounding rocket experiment shows no obvious disturbances under micro-g conditions [2,12]. Since the buoyancy differences under 10^{-4} g are negligible, the driving force for the droplet migration is reduced. As a consequence the phase L_2 will be incorporated at lower solidification velocities of the monotectic. No fluid flow in the melt was detected at the TEXUS-10 experiment. *7* *incorporated at lower solidification velocities*

Another variation in fluid flow exists in regions III and IV. After cooling under the consolute curve the minority phase will

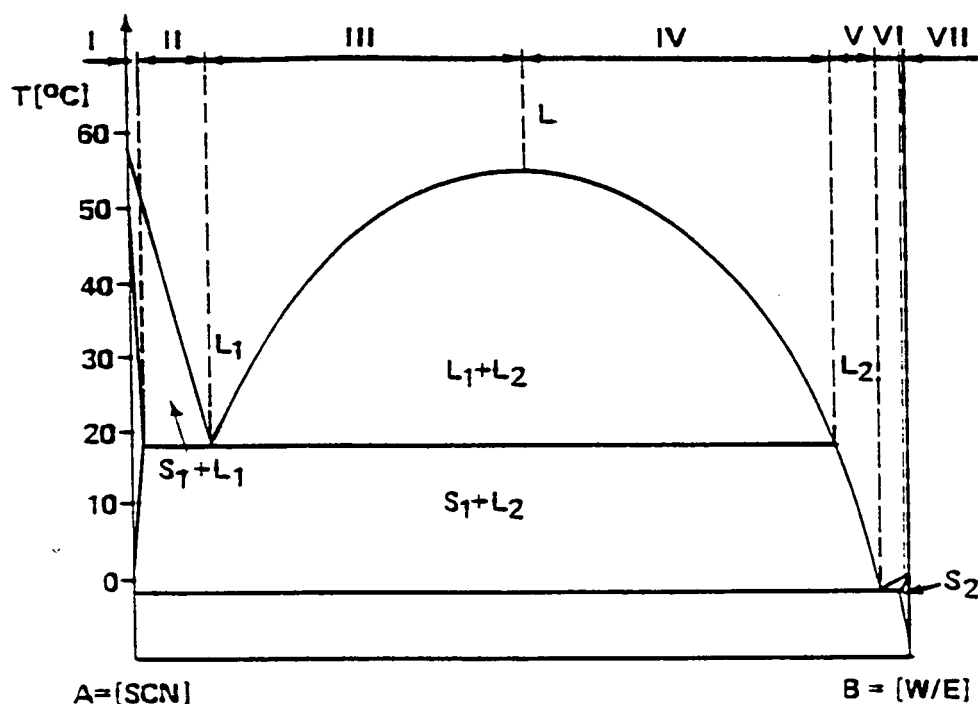


Figure 10: Principal phase diagram of a monotectic system divided into seven regions owing to the solidification and separation phenomena.

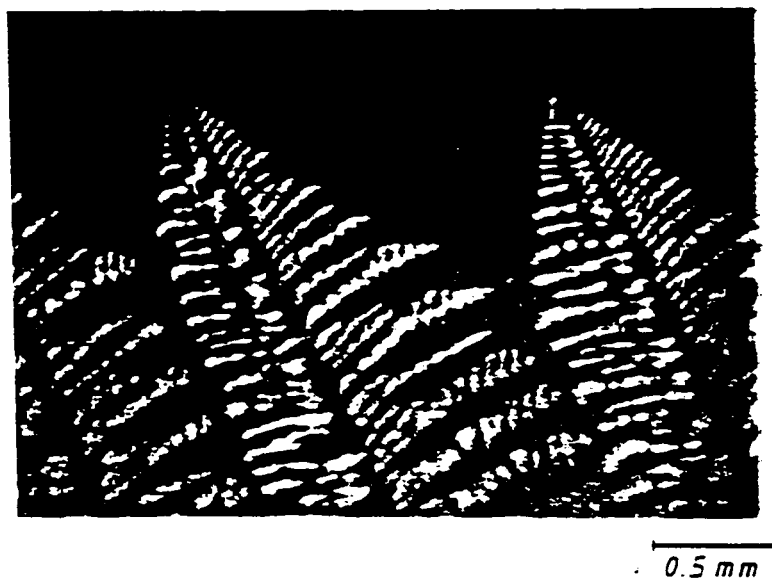


Figure 11: Growth of single dendrites in the organic transparent model system Succinonitrile-Ethanol, Ecker [2].

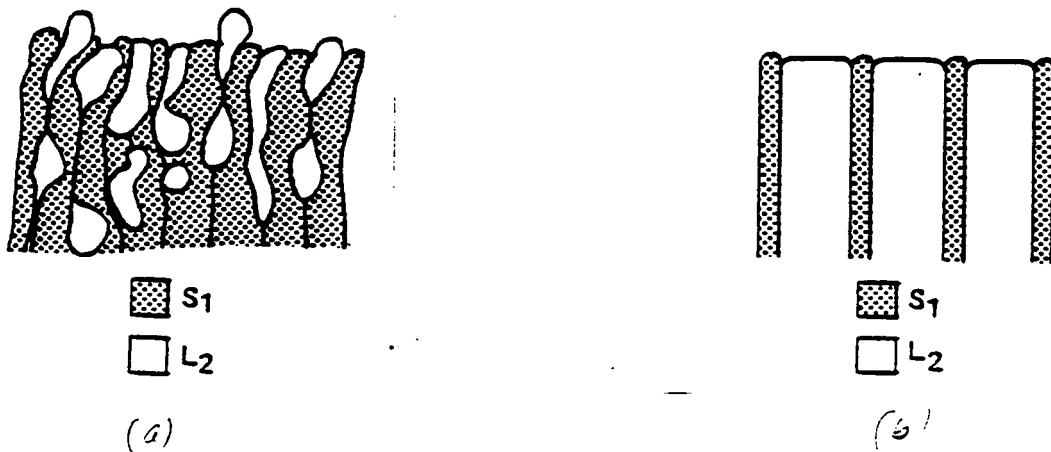


Figure 12: The monotectic interface growth will be unstable (a) or stable (b) depending upon the wetting conditions between L_2 and S_1 . For case (a) the liquid phase L_2 will be pushed or incorporated depending to the solidification velocity. For case (b), the liquid phase L_2 starts to rise driven by buoyancy, if in the liquid gaps at the monotectic phase will be a density inversion. Through the resulting pressure there will be the possibility to form droplets at the interface.

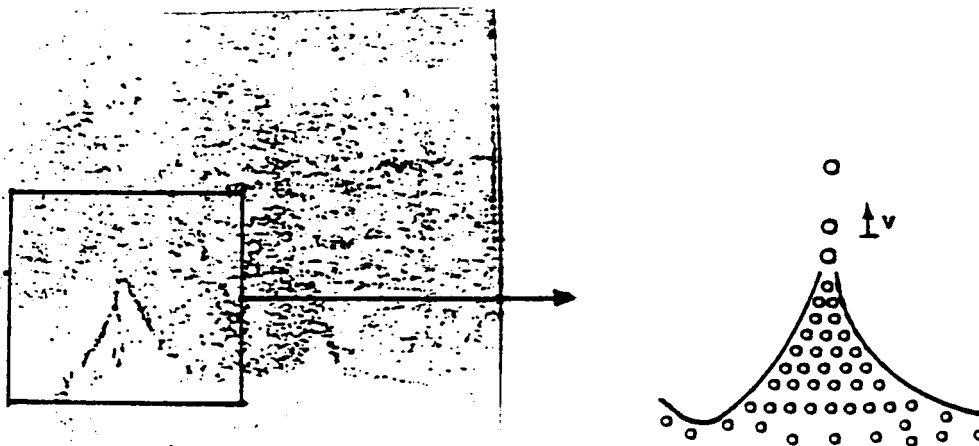


Figure 13: After a few minutes the flat cloud front will be deformed by rising droplets. A pyramidal structure was observed. The droplets initially migrate out of the center of this structure. Subsequently a plume like structure in the melt is established. These droplets transport substantial amounts of mass into the thermal gradient.

rising?

nucleate and form small droplets which grow by Ostwald ripening and coalescence while rising [13]. As soon as the initially flat cloud front is disturbed by the sing droplets the cloud-like interface will form a pyramidal structure, fig. 13. The tails associated with the rising droplets are positioned such that they lie directly above the apices of the pyramidal structure of the temperature profile near the interface. In the tail, the concentration of the minority phase is increased.

At region III we found in addition to the thermodynamic decomposition of the melt a decomposition owing to the monotectic solidification. The imperfect wetting condition causes "free" droplets of the E-rich phase at the monotectic solidification front to rise due to the large density difference between L_2 and L_1 . The size of the rising droplets is only dependent on the solidification velocity. The surface of the droplets is stable until the critical temperature of the consolute curve is passed. The droplets are driven by the same effects as in region II.

At region IV (system SCN-W) we found that in addition to the SCN-rich (L_1) droplets forming the plumes, there are larger volumes rising with a lower velocity in the same direction, fig. 14. The very slow motion of these W-rich volumes (compared to the W-rich droplets of region III) can be attributed to the fact that they are driven by buoyancy forces alone and do not have the additional driving force provided by thermocapillary effects. Similar conditions exist in the system SCN-E.

Careful observation and interferometric measurements indicate that the vertical alignment of rising droplets is a result of the interaction between the rising droplets and the surrounding melt. This interaction has two effects; firstly the local flow induced by the rising column of droplets results in the entrainment of droplets produced in the melt and at the solid-liquid interface; secondly each successive droplet will be subjected to less drag than the preceding droplet if it follows in the low pressure region behind the preceding droplet. The latter effect favors vertical-alignment.

This could well be one reason for the large difference between the theoretical velocity for droplet migration in a quiet melt and the experimental data. Because of the high number of rising droplets, there has to be a motion downwards. This motion pushes all droplets which start rising into this plume-like structure. Although droplets which start rising from the interface have to follow this plums. Both occurrences stabilize a plume-like structure in the melt. In addition, it is observed that the rise of groups of droplets is intermittent. We conjecture that this is a consequence of the fact that each droplet rises at a slightly greater speed than the previous droplet. As a result there will be periods of time when the plume is saturated with droplets. Addition of further droplets to the plume stops. Later when it is possible for droplets to move, the plumes reorganize and the

no run
for
well?
conclusion

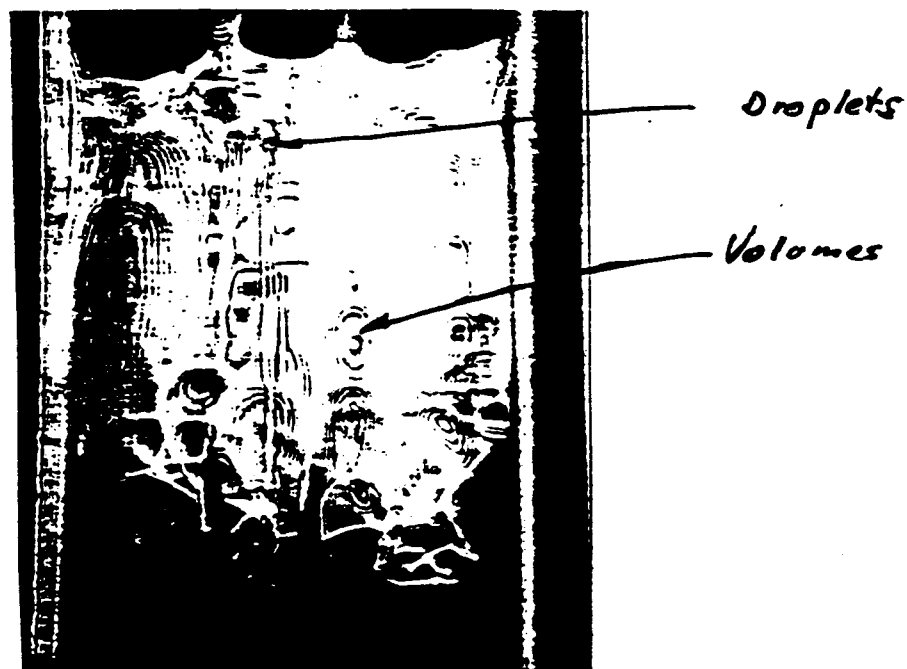


Figure 14: In region V two different flow phenomena were observed in the melt. In addition to the thermodynamic decomposition of the melt rising volumes of the majority phase were observed.



(a)



(b)

Figure 15: In region VI slowly rising volumes of liquid were observed. Only a few migrating droplets were measured.

(Shadowgraph (a); hologram (b))

process repeats itself. Only a few percent change shifts the phase diagram back into the miscibility gap. The complexity of the motion in the melt at region IV is indicated by one example in table 2.

It was possible to isolate this rising volume phenomena using an alloy composition of region V, fig. 15. A primary thermodynamic decomposition is only present in this region if the liquid is undercooled below the extended consolute curve. (A low number of small droplets originate then in the water-rich phase L_2 .) Other motions in the melt could only be induced from the liquid phase L_2 in the interdendritic gap in front of the eutectic phase. The moving volumes consist of the phase L_2 and are driven by the concentration difference. The density inversion in the W-rich phase will cause an additional driving force.

For all experiments it was very important to homogenize the melt at a higher temperature as the maximum gap temperature with convective stirring. In these relatively large samples homogeneity was not achieved by diffusion after 15 hours in the melt. Figure 16 shows the diffusion profile resulting from two SCN-rich droplets at the bottom of the sample. First, the sample from region V was solidified after which all facilities were switched off. The sample with SCN-91.8wt% W was then held at 25.8°C for 15 hours. Only with the help of convection ^{was} homogenization ~~was~~ successful. This decomposition during melting of a monotectic alloy establishes different concentration boundary conditions at lg and micro-q conditions.

Homogenization through convective stirring is impossible in existing furnaces under micro-g conditions. This incomplete homogenization through the melting procedure may be one reason for inconsistent solidification behavior from monotectic solutions in micro-g.

The results of the work are summarized in table 3.

ACKNOWLEDGMENT

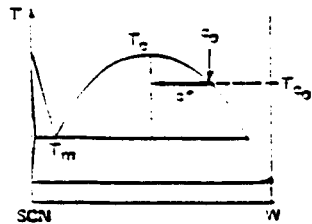
The author gratefully acknowledge the European Space Agency (ESA) for supporting this research and the National Aeronautics and Space Administration (NASA) for making available the experimental facilities.

LITERATURE

- [1] Schreinemakers, F.A.H.
Zeitschrift f. phys. Chemie, Bd. 23 (1897) and Bd. 26
(1898)

Table 2: The complexity of the phenomena in a solidifying monotectic is illustrated with this example.

Boundary conditions:



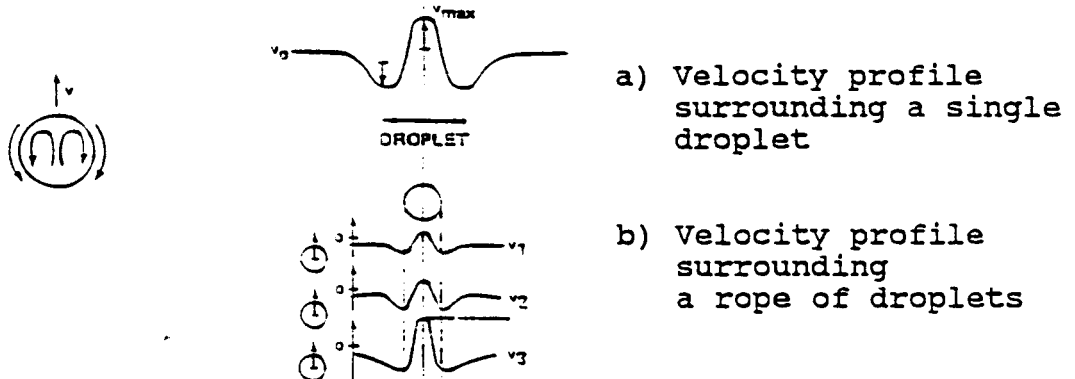
- System SCN-W
- $c_0 = \text{SCN-60wt\% W}$
- $T_{D0} = T_M$
- $T_{Dy} = T_M$
- $c_D = c(T_{D0})$
- coordinate system

Step 1: Cooling under the consolute curve.

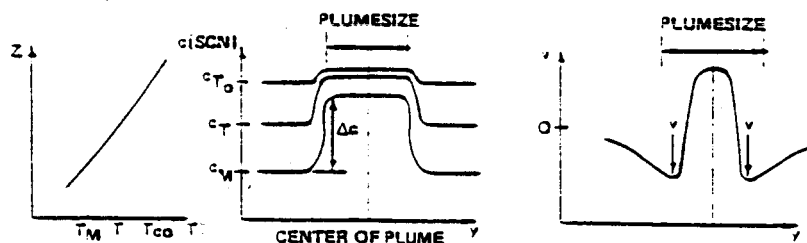
- > Phase separation in the melt. SCN-rich droplets (higher dense, than surrounding melt) migrate up the temperature gradient.

Step 2: SCN-rich droplets establish a plume-like structure in the melt.

- > Fluid flow down from the top of sample.



Step 3: Influence on the concentration profile



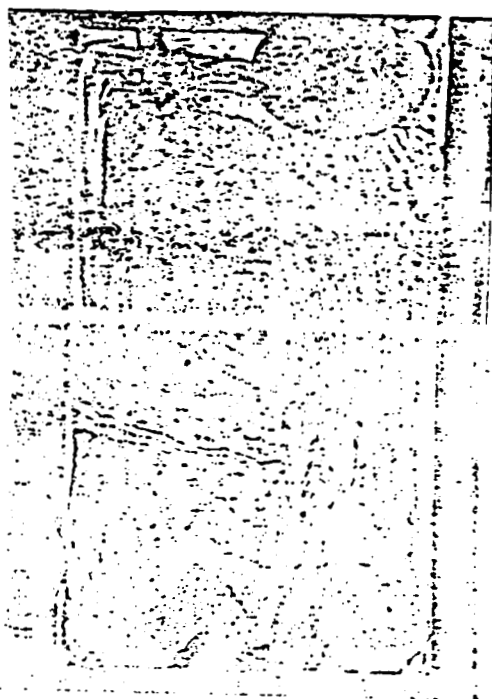
If $c^* < \Delta c$, then melt near the plume is so highly super-saturated, that $c_0 - \Delta c < c_c$. c_c is the concentration associated with the maximum monotectic gap temperature.

- > Concentration shift near plume from region IV to III.

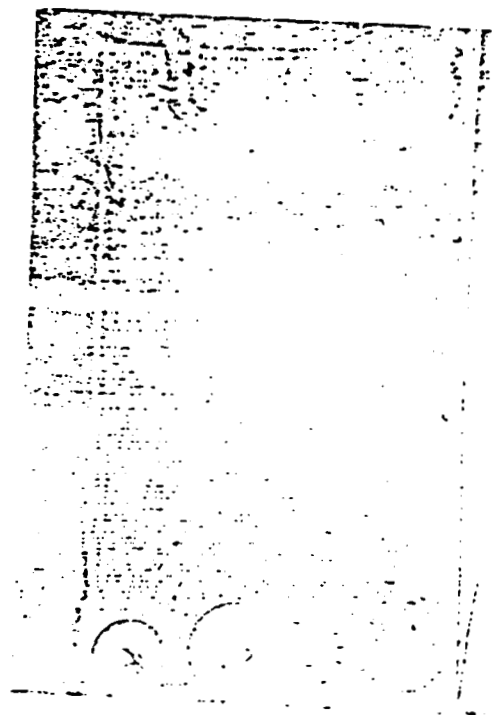
Fluid flow downwards near the plume transports the super saturated melt into cooler regions. Thermodynamic decomposition of the melt creates W-rich droplets, which are formed from the downward moving fluid. They are only stable in the supersaturated region.

- > SCN concentration near the plumes and W concentration near the s-l interface will be increased.
- > Stabilization of the plumes. Parallel reduction of the SCN concentration near the s-l interface.
- > Decreasing number of SCN-rich droplets.
- > Plume destruction by diffusion following cessation of fluid flow.
- > Favor W-rich droplets migrate down.
- > Increase of SCN concentration and the cycle is repeated.

Index: D = Droplet; m = monotectic; M = melt; R = radius



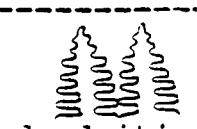

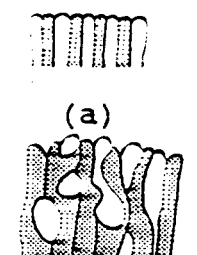
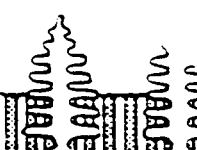
(a)

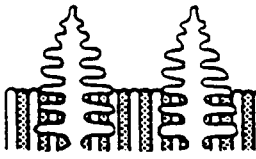
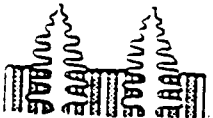
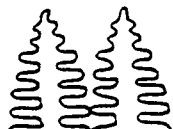


(b)

Figure 16: Remelting of a solidified monotectic does not necessarily lead to a homogenized melt. The latter may be achieved only by convective stirring (a). After 15h at 25.3 C the inhomogeneity in the melt, owing to the melting process was observed (b), (SCN-94wt% W).

Table 3: Summary of flow phenomena in the melt of monotectic systems.

Part Solidification Front	Decomposition in the melt	Decomposition by solidification	Remarks ($G_T < m_1 * G_C$)
I  dendritic	no	no	Convection only if $Ra_C > Ra_T > Ra_{min}$ [14]
II  inter-dendritic monotectic phase	W/E-rich droplets only, if melt is under-cooled under the extended consolute curve. Droplets migrate due to buoyancy and thermocapillary force.	W/E-rich droplets observed, if cooled under the monotectic temperature.	Monotectic phase : - Separation of the E-rich phase owing to the non wetting condition. Droplet incorporation is function of solidification velocity. - Separation of the W-rich phase owing to the density inversion. The L_2 wets the S_1 phase.
III  (a) (b) stable (a) or unstable (b) monotectic	Fog in front of s-l interface associated with a pyramidal structure. W/E-rich (less dense) droplets associate with a pyramidal structure. Droplets migrate in plumes. Driving forces: Buoyancy and thermocapillary effect.	W/E-rich droplets observed.	Monotectic phase : - Separation of the E-rich phase owing to the non wetting conditions. Droplet incorporation is a function of solidification velocity. - Separation of the W-rich phase owing to the density inversion. The L_2 wets the S_1 phase.
IV  interdendritic eutectic phase	Fog in front of s-l interface; SCN-rich (high dense) droplets associate with a pyramidal structure and a plume-like configuration. Driving force: Thermocapillary convection countered by opposing buoyancy force.	W/E-rich migrating volumes (less dense) Driving force: Buoyancy	

V  inter-dendritic eutectic phase	SCN-rich droplets possible, if high supersaturation in front of the s-l interface. Driving force: Thermocapillary countered by opposing buoyancy effects.	W/E-rich migrating volumes (less dense). Driving force: Buoyancy.	
VI  inter-dendritic eutectic phase	no	no	convection only, if $Ra_C > Ra_T > Ra_{min}$
VII  dendritic	no	no	convection only, if $Ra_C > Ra_T > Ra_{min}$

with: Ra_C = solutal Ra-number $f(D, c)$, Ra_T = thermal Ra-number $f(\alpha, T)$
and Ra_{min} = critical Ra-number

- [2] Ecker, A.
Dissertation, University of Aachen (RWTH), West-Germany
1985
- [3] Smith jr., J.E., Frazier, D.O., Kaukler, W.F.
Scripta Metalurgica, Vol. 18, P 667, ()
- [4] Grugel, R.N. and Hellawell, A.
Met. Trans., Vol. 15 A, 1984, p. 1626
- [5] Young, N.O.; Goldstein, J.S. and Block, M.J.
J. Fluid Mech., Vol 6, 1959, p. 350
- [6] Facemire, B.R.
personel communication, t.b. published
- [7] Lacy, L.L., Nishioka, G.M., Facemire, B.R. and
Witherow, W.K.
NASA TM - 82494, June 1982
- [8] Frazier, D.O., Facemire, B.R.
personel communication, t.b. published
- [9] Sahm, P.R. and Ecker, A.
Z. Metallkde., Bd. 75, H. 5, 1984, p. 325
- [10] El-Wakil, M.M. and Ross, P.A.
Progress in Astronautics and Rocketry, Vol. II,
Academic Press, New York 1960
- [11] Mayinger, F. and Panknin, W.
Proceedings of the Int. Heat Transfer Conf. Tokio 1974
- [12] Ecker, A. and Sahm, P.R.
to be published
- [13] Baird, J. and Frazier, D.O.
to be published
- [14] Turner, J.S.
Cambridge, University press (1973)